A Linear Mode within Non-linear Structure enhances On-Orbit Calibration for 6 dof space force sensing tool.

Sherry Draisey, Good Vibrations Engineering Ltd., sherry@gve.on.ca

ABSTRACT

There were over 10,257 satellites Earth Orbit: 8033 Low Earth Orbit (LEO), reported for 2024 on the website: Orbiting Now.

Satellite servicing is going to be actively pursued – if only to gather up bits and drag some of them out of the way. Space robotic force sensing is already being employed for some servicing operations.

The space robotic force sensor prototypes described in this design employed segmentially poled piezo ceramic elements, internal to the non-linear sensor structure. The active application uses low level internal vibration. It affords the ability to monitor multiple types of motion (rigid body, flexible quasi-static and flexible dynamic) for each of 6 sensing degrees of freedom (6dof). The structure's non-linearities allow for load measurement based on resonant frequency shift. The shapes of modes identify the force dof being excited. The ability to measure multiple modes for sensing dof offers the advantage of averaging results to improve accuracy.

The nature of the structural configuration also creates linear modes – not influenced by externally applied loads. The linear modes do not contribute to force measurement resolution, but they are useful for sensor calibration. This paper reviews FE and test results of 2 prototypes to validate the lowest mode linearity.

The presence of piezo ceramic active element predominantly excites modes involving the loading plate. It is these modes which have been rendered non-linear by the presence of pin-ended strut elements. The non-linearity influences caused by strut rigid body angular deflection influence load path, offering force transduction capability. The centrally located piezo-ceramic element also excites 'housing modes', which tend to be linear (the example being discussed here includes excitation of the housing base plate). As the piezo is driven, its expansion and contraction take place at both ends of the piezo element (as well as a small diameter Poisson's ratio effect).

Introduction

This paper investigates a linear mode of the structure, based on test results of loads applied to each of two different size FMS prototypes. There is also a finite element (FE) model for each prototype, which offers more detailed description of the first linear mode shape of prototypes 2 & 3. The linear mode is referred to as a housing mode. The goal is to confirm that one of the lower modes of the structure is independent of applied external load.

The loading conditions for the 2nd prototype extended to larger amplitudes than that of the 3rd prototype, but the 3rd prototype included low levels of applied torsion loads. The discrimination between applied load degrees of freedom and excited modes is important.

The means of sensing of resonant frequencies of the two prototypes is different (2nd prototype is based on cross axis piezo response voltage, the 3rd prototype measurement is based on accelerometer response). Both have been correlated to their respective FE. The focus on a linear mode is based on its usefulness for on-orbit calibration.

Force Sensors

This report is based on results from two different prototypes, mentioned as the 2nd and 3rd prototypes. Each of these sensors were based on using segmentially poled ceramic elements to excite dynamic response. The 2nd sensor was a large diameter sensor, the 3rd was much smaller, but they are both in fundamentally the same configuration (Figure 1). The sensing elements for each were different. The 2nd prototype based on cross-axis voltage response did not provide shape information but the 3rd prototype measurement accelerometers did.

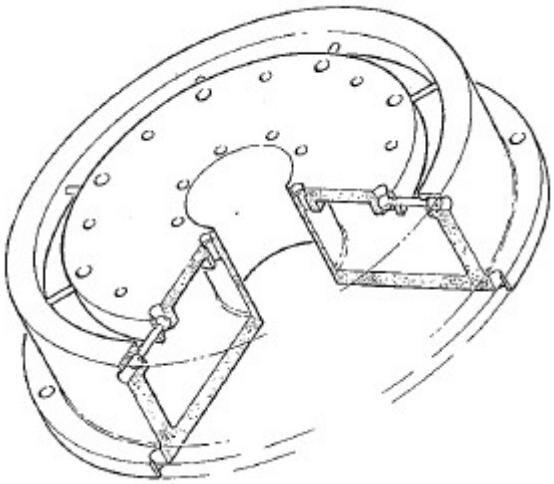

FIGURE 1: MECHANICAL CONFIGURATION FOR PROTOTYPE 1 (Draisey, 2016)

2nd Prototype Force Sensor

Mechanical Configuration

The 3 dof force and moment sensor breadboard is pictured in Figure 2 (Draisey, 2003),. The loading plate changed from prototype 1 to be solid, without a central hole.

Loading plate – a 12" diameter, 0.5" thick aluminum plate with 8 locations for strut/cable attachment equally spaced along circumference.

Housing – 15.25" diameter, ¼" thick, 2" high, hollow cylinder, one end closed

Struts – the struts steel threaded pin ended rods, with ball threaded onto end inserting into housing and loading plate at each end.

Piezoceramic element – a hollow cylinder (Sensor Technology, BM400 cylinder), 2" diameter, 1/8" thickness, 1" high is segmentially poled into 4 quadrants. The element is driven to small amplitudes (~0.08g's) at a multitude of loading plate resonances. The sequence of element drive is varied to ensure modes of significance are excited.

FIGURE 2. PHOTOGRAPH OF 2ND PROTOTYPE (3 DOF) SENSOR

3rd Prototype Force Sensor

Mechanical Configuration

Figure 3 shows 3rd prototype sensor cross section.

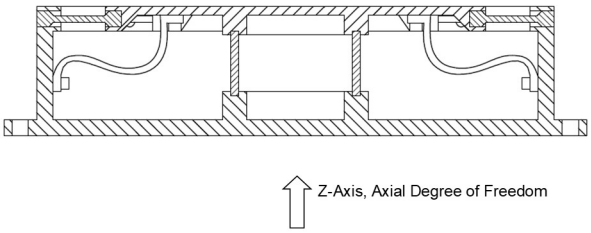

FIGURE 3. 3RD PROTOTYPE FORCE SENSOR CROSS SECTION

Loading plate – a 5.875” diameter, 0.125” thick aluminum plate with 8 locations for strut/cable attachment equally spaced along circumference.

Housing – an 8” diameter, 2” high, hollow cylinder, one end closed. The other end has strut/cable attachment fittings, spaced along open end circumference. The closed end of the cylinder has a 9” diameter flange.

Struts/cable – the current design is based on slightly tensioned cables, rather than pin-ended struts. There are to be 8 0.1” diameter cables, which act to join the loading plate with the housing. The finished cable + end fitting length is 1.4375”. The cable ends are swaged into end fittings which are counter threaded to allow for changes in the nominal preload

Delrin inserts – there are 2 hollow delrin cylinders to position the piezoceramic element between the housing based and loading plate. The ceramic element was glued into grooves. The delrin is to ensure electrical isolation and reduce wear on the ceramic element pole.

Piezoceramic element – a hollow cylinder, 2” diameter, 1” high is segmentially poled into 4 quadrants. The element is driven to small amplitudes (~0.08g’s) at a multitude of loading plate resonances. The sequence of element drive is varied to ensure modes of significance are excited.

Thermal straps - 8 thermal straps connect the loading plate to the housing walls. They reduce the thermal gradient.

The struts generate the non-linearity. There are 3 regions of non-linearity, which we have identified from correlation between experimental and analytical results with our 2nd prototype. The non-linear mode shifts have been established (Draisey, et al., 2003).

Figure 4 shows the segmentially poled ceramic element, also shown in Fig. 3, joining the upper loading plate to housing base.

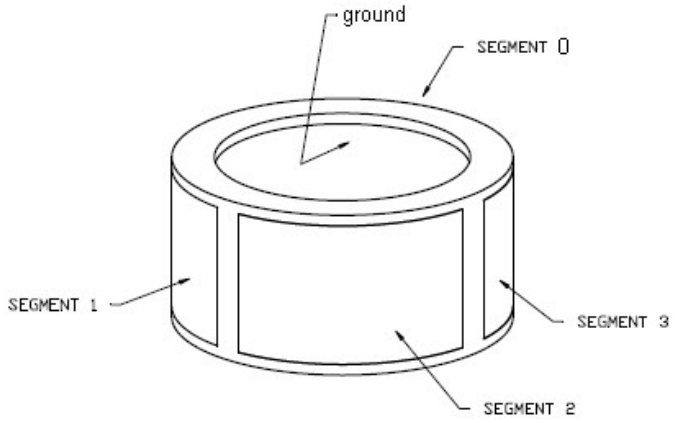

FIGURE 4: SEGMENTIALLY POLED CERAMIC ELEMENT

Experimental Power Subsystem

Power is provided for 3 subsystems:

accelerometers: 5V

AC/DC 5V adaptor for BeagleBone microprocessor

3.3V generated to run drive electronics.

Data transferred from microprocessor to a PC running either Matlab or Excel.

Sensor Instrumentation

Not all sensor motions are tested for. In the 2nd prototype, it was piezo ceramic element voltage, which was measured, which corresponds to dynamic strain, and for the 3rd prototype, it was acceleration. The quasi-static deflections were not measured for either prototype.

The loading plate experiences 3 kinds of deflections, under applied load. They are show in cross axis view of ½ loading plate, outboard of piezo, Figure 5.

- Static, due to externally applied load - green
- Rigid Body, due to the piezo drive – blue
- Dynamic Response, created by piezo action - red

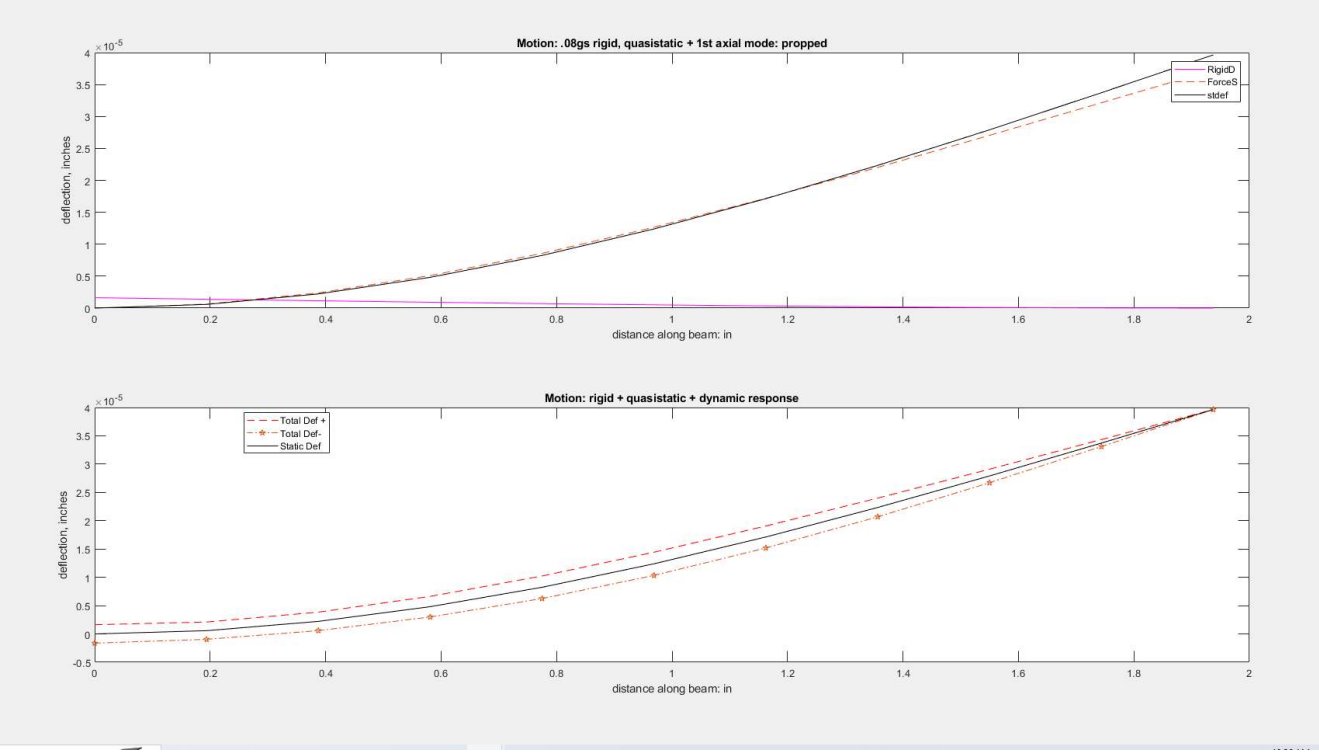

FIGURE 5: STATIC AND DYNAMIC DEFLECTIONS ON LOADING PLATE for A SMALL AXIAL LOAD

The FE modelling was all done with normal modes analysis. The test results are dynamic responses. They are similar in frequency and shape, because of the low damping values and type of load applied through the piezo.

There are several small deflections that occur at the loading plate, which modify the dynamic response. Figure 5 gives an indication of their relative amplitudes for the first mode of the loading plate. The green one includes any static deflection that a small

external load would create, and the other is the rigid body influence if all 4 piezo segments were driven in phase. The dynamic response is dominant, but the dynamic shape, including static deflection of applied load produces a dynamic shape which is no longer symmetric.

2nd Prototype Sensor Instrumentation

The response voltage of the non-driven poled ceramic elements was monitored, filtered and acquired through Keithley DAS-1800 ST/HR Series. It was then fed into Matlab to note resonant frequencies. This method of data sensing limits determination of cross axis response to Z dof excitation. The driven axis segments (for example segment 1 and segment 3, measured for segments 2 and 4). They were driven either together, in phase to generate axial modes and out of phase to generate moment modes.

3rd Prototype Sensor Instrumentation

Five 3 axes LSM6DS33 accelerometers, capacitance set to allow maximum frequency of 2500 Hz. Though they don't meet the maximum frequency requirement, they are adequate to validate at least one mode for all 6 force degrees of freedom. The higher frequency modes were validated, for breadboard work, using 2 existing in-house Dytran accelerometers. Table II shows the expected frequency range of all modes.

Figure 6 shows the axis system and drive segment orientation and accelerometer placement on under side of loading plate. Data transferred from Beaglebone microprocessor to PC running either Matlab or Excel.

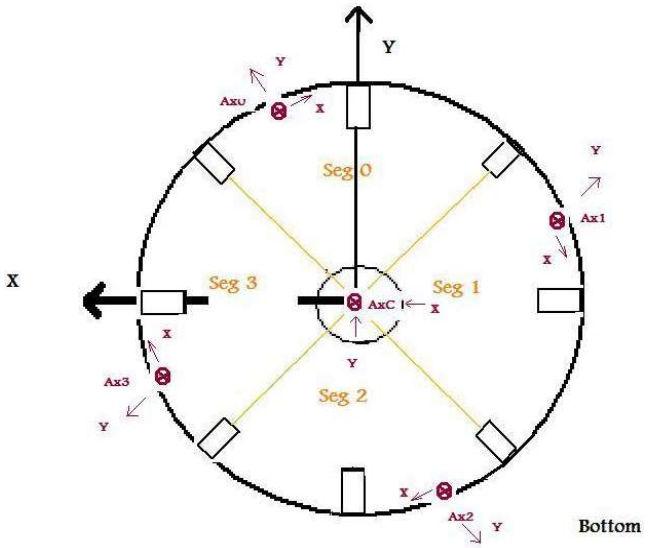

FIGURE 6 INSTRUMENTATION ON LOADING PLATE

.

Finite Element Analysis

2nd Prototype Sensor Model

The finite element modelling has been done using UAI NASTRAN. The predictions for this project are based on linear static, temperature and normal modes analysis, though earlier nonlinear investigations have been made.
The model consists of:

housing (112 plate elements); piezoceramic sensor (64 plate elements); loading plate

(16 solid elements + 17 plates); struts (8 beam elements). There is a total of 210 grids. The model is shown in Figure 7.

The initial model had 8 three dof single point restraints (SPC), representing the 8 bolts mounting the structure to the test rig. This initial analysis uncovered a pair of unimportant housing modes in an already heavily clustered set of significant non-linear modes. The FE analysis was used to eliminate this pair of unimportant modes (1725 Hz) with the addition of 8 more three dof SPC's. This modification was implemented in the hardware (with the addition of 8 bolts).

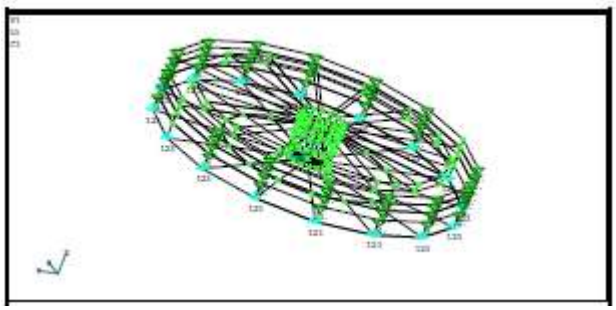

FIGURE 7 2nd PROTOTYPE FE MODEL

2nd Prototype Sensor Results

The test verification of the structure was largely limited to modal frequency predictions up to 2000 Hz. The model was fairly accurate without modifications (Draisey, et al., 2003).

Table I presents the frequencies for the FE predictions (linear, representing unloaded condition) and the test frequencies that upgrades were targeted to. Not all test frequencies could be taken as reliable, because they were based on measurements taken with the cross-axis piezoceramic element response. The piezoceramic element's position at the centre of the structure could not capture all modes well. Only one test mode is identified for each orthogonal pair of modes. The pair of modes at around 1725 Hz were identified in the model, as well as in the test results. This pair was successfully removed (they were obscuring the identification of frequency shifts occurring in 1800 to 1900 Hz range.

TABLE I 2ND PROTOTYPE PREDICTED FE MODES (AFTER UPDATE)

Mode Number	Test Measurement Freq (Hz).	FE Predictions		
		Freq (Hz).	Tube ε	shape
1	250.0	271.0	0.95	1st upper plate
2	301.5	305.5	7.08	upper plate rot
3		305.8	7.07	upper plate rot.
4	440.	497.1	75.6	tube rotation
5	600.	645.4	0.66	piston in housing
6		699.1	0.38	upper plate saddle
7		699.7	0.36	upper plate saddle
8	950.	1205.5	6.22	up. plate rot.
9		1206.1	6.21	up. plate rot.
10	1377.	1584.2	2.49	bottom plate mode
11	1547.	1657.9	3.50	upper plate
12		1658.6	3.57	upper plate
13	1900.	1817.1	25.8	housing & plate
14		1817.2	25.8	housing & plate

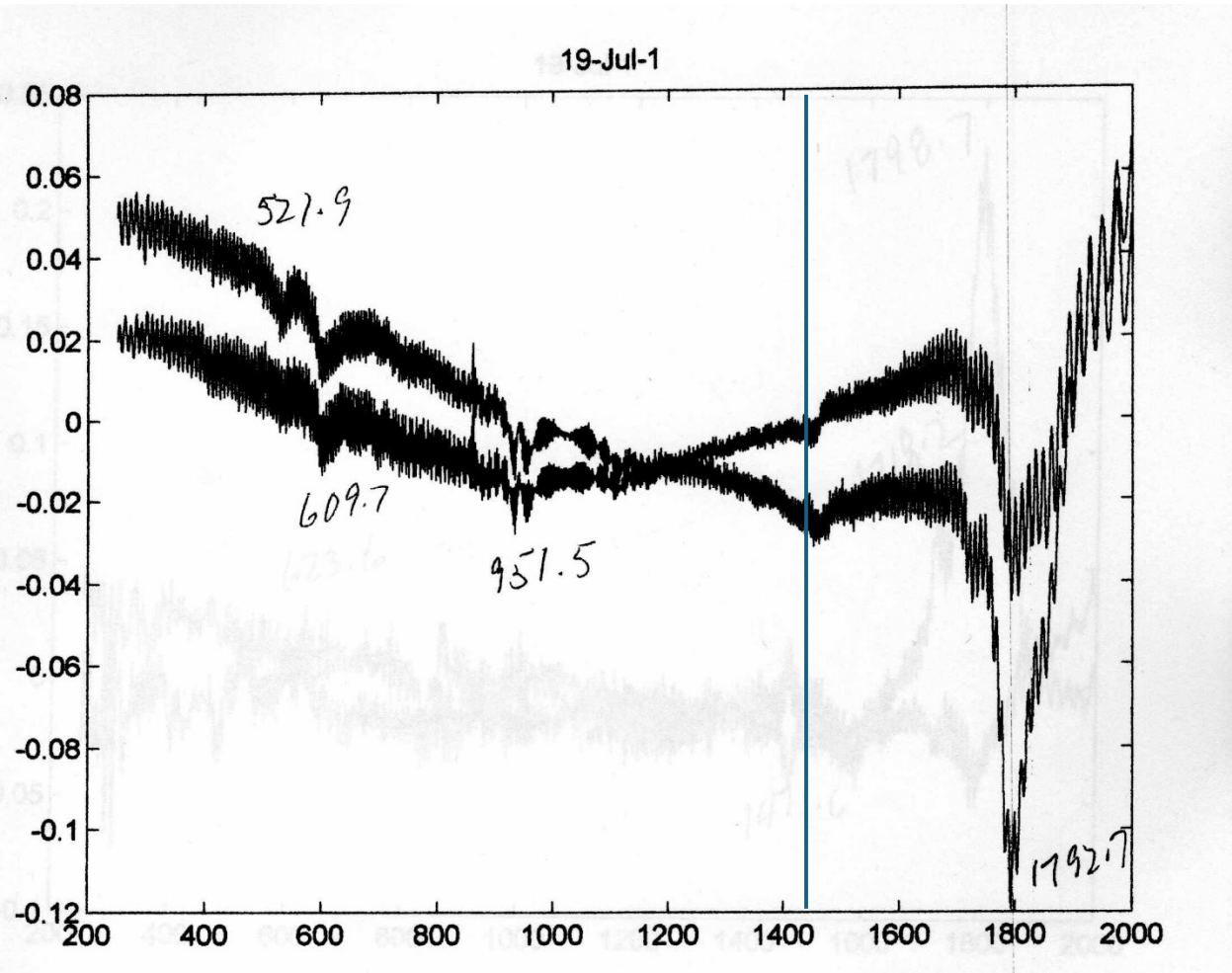

FIGURE 8 AXIAL DRIVE, NO APPLIED LOAD

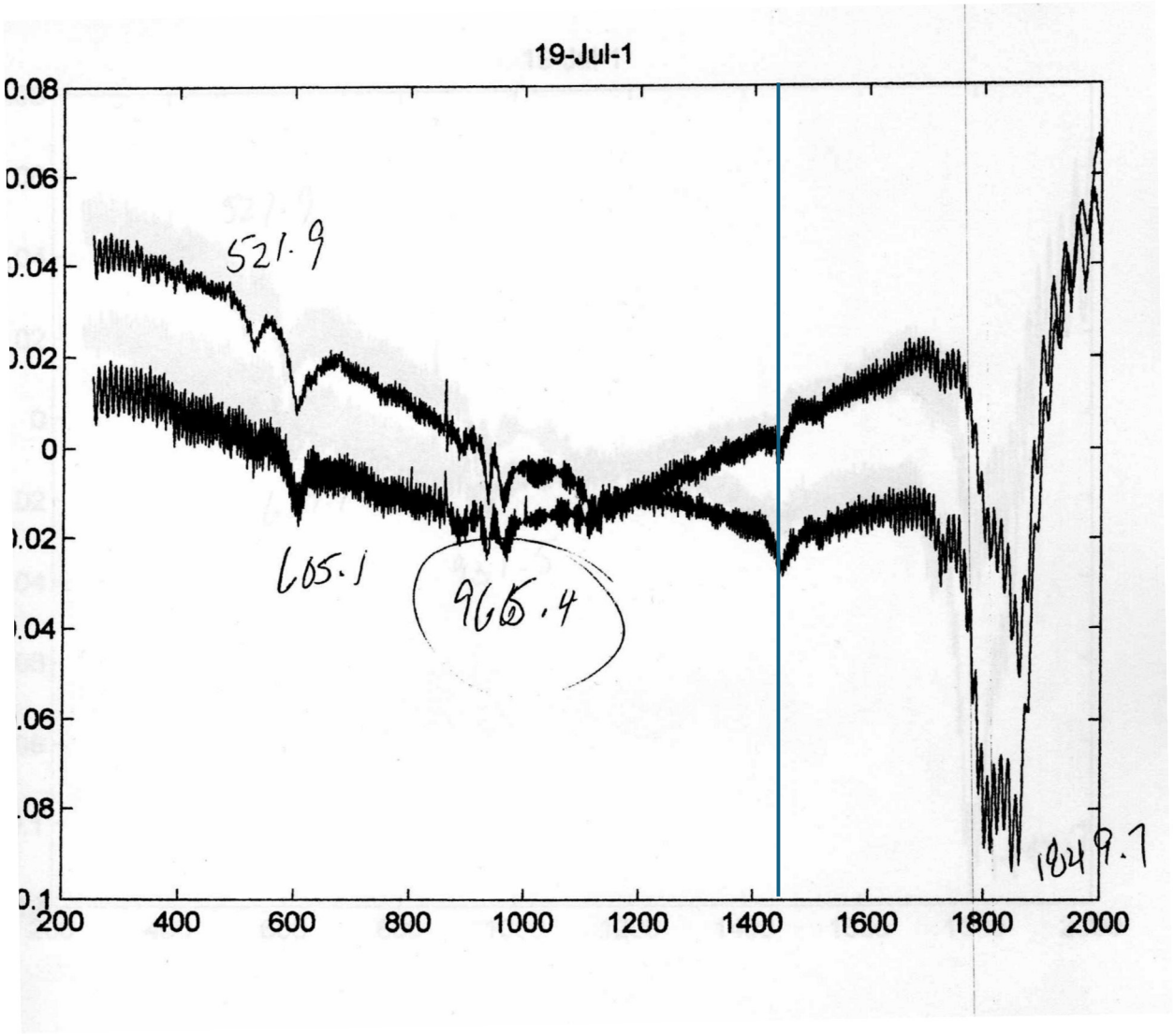

FIGURE 9 AXIAL DRIVE, 10 KG APPLIED LOAD

3rd Prototype Sensor FE Model

A simple UAI Nastran finite element model (340 grids, 312 structural elements: 40 bars, 272 plate elements and 12 concentrated masses). The mass is 3.6 lb (1.64 kg.). The model has been run repeatedly to determine baseline eigenvectors. These results are shown in Table II It has also be run for geometric stiffness influences, expected for applied static loads.

Figure. 10 shows the loading plate portion of the FE model. Initial runs were based on loading plate with central hole, but then it was upgraded to reflect a filled center. The filled center is an important development for the lowest frequency linear mode, targeted in this paper.

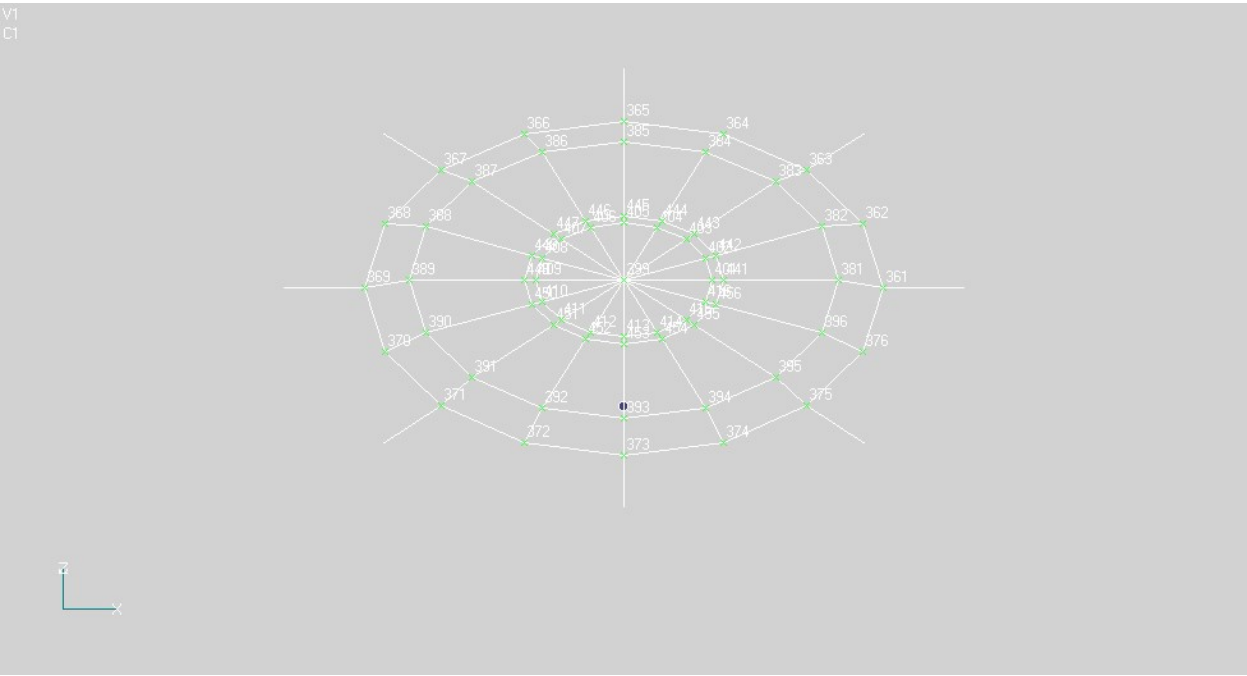

FIGURE 10: FE MODEL OF 3rd PROTOTYPE LOADING PLATE & STRUTS

3rd Prototype Sensor FE Results

The FE results presented in Table II. are taken from eigenvector analyses in four different linear configurations – two with the struts (axial load capability only), the other two with the struts as they would present for loaded out of load plate plane or in plane (deformed by

externally applied load) configuration. The first column of each group is the resonant frequency; the 2nd column is the dominant participation factor for that mode. Participation Factor is an indicator of mode shape (Draisey, et al., 1985).

For example, the first column, 2nd row (rocking dof), shows a minimum frequency of 655 Hz, and a maximum frequency of 814 Hz (column 3). Both have RY dominant participation factors ~3.80. The 655 Hz reflects the frequency that would be measured if no load of any type was on the structure. The maximum frequency of 814 Hz. reflects the measurement if a load 12.7 Nm (112.6 in-lb) was being applied.

3rd prototype Sensor FE Results

Table II

Freq (Hz)	**8 struts,**	**Freq**	**8CBARs 456-45**	**Freq**	**8CBARs 456-46**	**8 struts**		**Shape**
8 SPC's	Dom PF	8 spc's	dom PF	8 spc's	Dom PF	16 spc's	Dom PF	
655	RY=-3.76	778	Z=1.764	655.4	X=-.31,RY=-3.77	736.1	Z=1.86	axial
655	RX=3.76	814.2	X=.31, RY=3.83	655.7	Y=-.31, RX=3.76	738.6	RY=3.85	rocking
686	Z=1.81	814.2	RX=3.82	686.5	Z=1.81	738.6	RX=3.85	rocking
988	Z=-.002	1052.1	RZ=-3.54	988.6	RY-8.5e-3	1157.3	RZ=3.55	torsion
1052	RZ=3.54	1089.8	RZ=-2.5e-3	1053.7	RY=1.3e-3	1160.4	Rz<10e-10	rocking
1053	RZ=-.04	1163.3	RY=1.44e-3	1139.5	RZ=3.55	1160.4	Rz<10e-10	rocking
1209	Z=.96	1241.1	Z=-.81	1208.7	Z=.96	1262.7	Z=-.9	housing
1730	RX=.18	1794.5	Y=-.06,RX=.23	1729.8	Y=-.05,RX=.18	1966.6	Y=-3.45e-8	shear
1730	RY=-.18	1794.5	X=-.06, RY=-.23	1729.8	X=-.05, RY=-.18	1966.6	X=3.45e-8	shear
2737	Z=-.04	2737.9	RY=1.6e-3	2738	Z=-.04	3015.9	Rz=8.4e-9	4up, 4down

SPC= single point constraint
CBAR is a beam element (UAI, 1999)

The predominantly linear mode (independent of loads applied through loading plate) is highlighted in orange. It is quite sensitive to external boundary conditions, but not to the internal ones which transfer some load from upper loading plate to outer housing. The model cross section demonstrating the load path for mode 7 is shown in Figure 11. It includes: the load plate in red, the piezo-ceramic element in blue and the base plate in purple. The deflected shapes are dashed. The external boundary conditions represent 16

bolt connection (3 dof SPC's) and 8 strut connections (no rotational restraints at either end of 8 beams) between loading plate and housing.

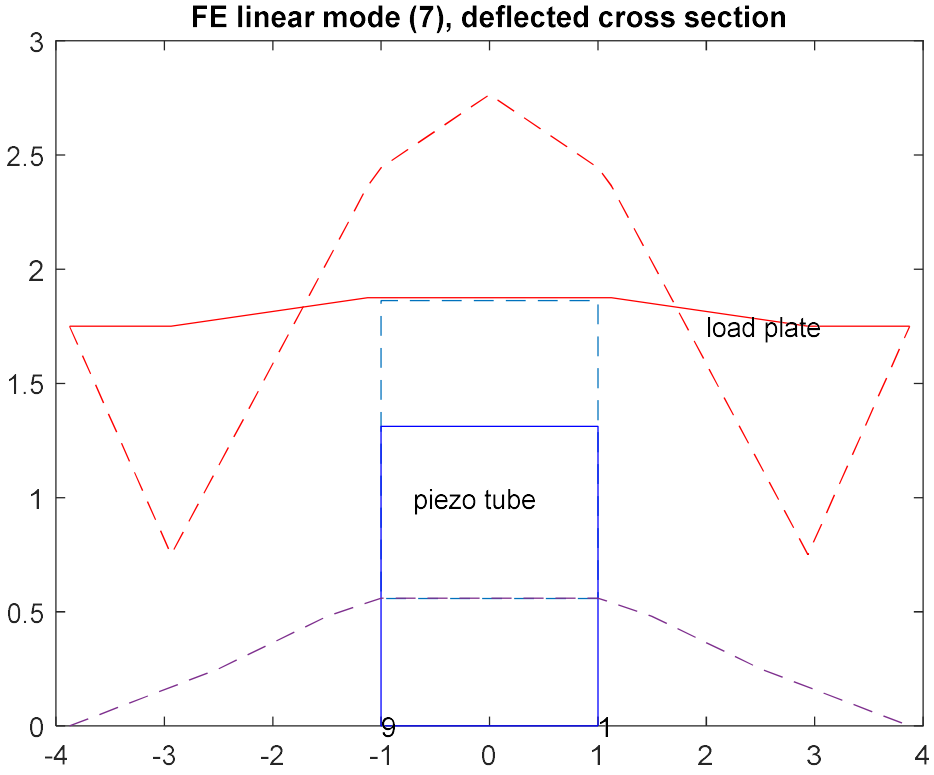

FIGURE 11, Cross Section of FE model; Deflected and Undeflected Shape

Figure 12 shows 2 accelerometers responses to sine sweep, with drive of 2 opposing piezo ceramic elements (1 and 3 phase shifted by 150^{0}) excited mostly as rocking motion (Draisey, 2020). The Poisson's ratio produces enough shear influence to excite the torsion mode.

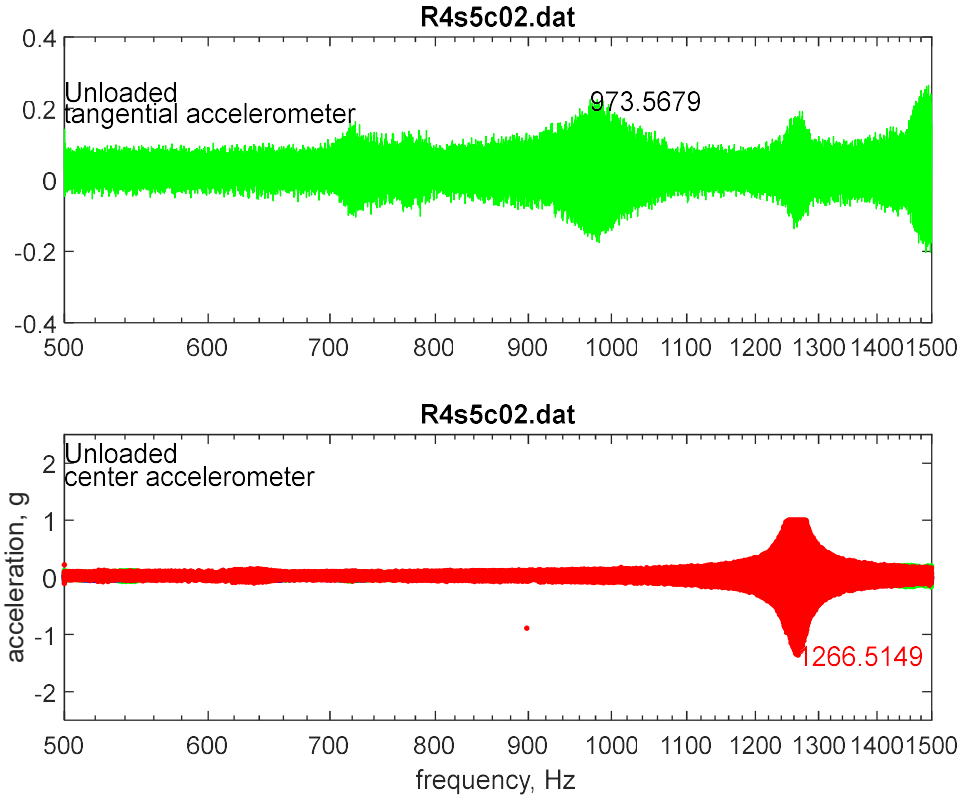

FIGURE12, ACCELERATION VS FREQUENCY; ROCKING DRIVE
NO EXTERNALLY APPLIED LOAD

The upper figure 12, in green, shows a tangential accelerometer (located at perimeter of loading plate) response. The torsion mode is the peak shown at 973 Hz. The lower figure, in red, shows the central accelerometer, on loading plate, Z axis response. The central accelerometer is the peak response for this mode at 1267 Hz. The upper portion of the red response has been electronically clipped. At the time of experimentation, there was no interest in this linear mode, so no effort was made to correct the situation.

Figure 13 shows the FE mode 7 loading plate shape and test result shape from accelerometers on the loading plate only. The test results for this shape were about 1266-1268 Hz, loaded or unloaded. The test results varied from day to day (though not within any single day). FE investigations noted that the external boundary conditions were significant, and between each testing day, the structure was often moved out of the way.

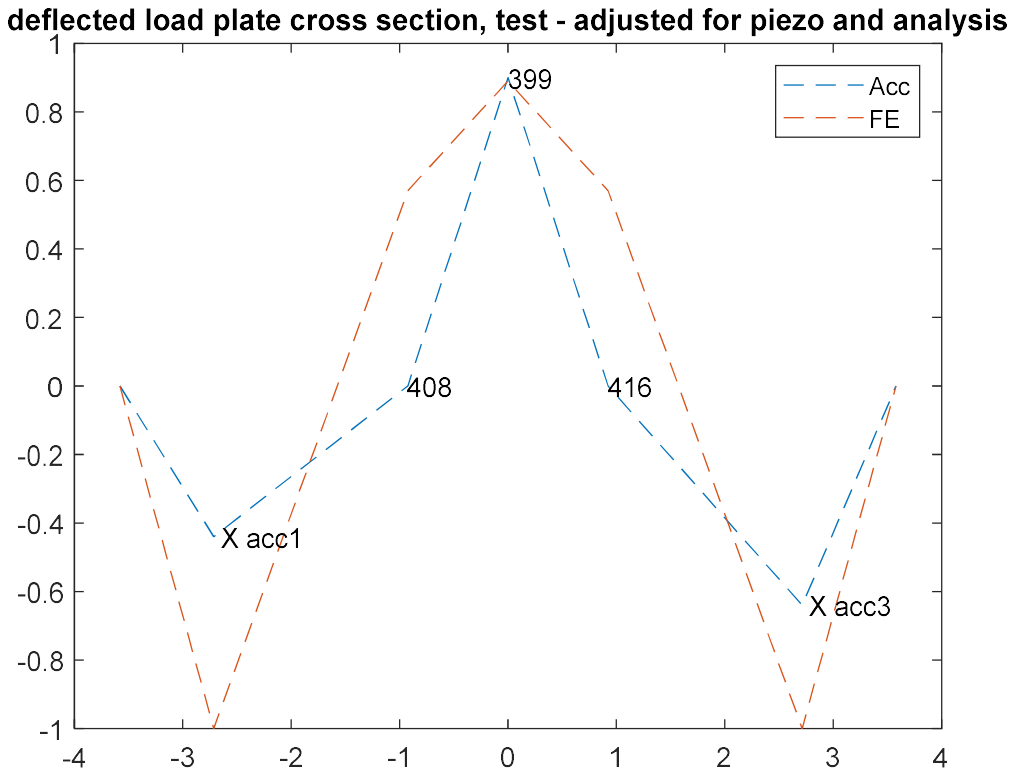

FIGURE 13, CROSS SECTION OF LOADING PLATE: FE MODEL AND TEST ACCELEROMETERS

Results for Prototypes

Table III shows both FE and test results for the 2nd and 3rd prototypes. The linear mode of this paper is highlighted in yellow.

The 1st prototype was quite similar in mechanical configuration to the 3rd prototype, except it did not utilize a piezoceramic element to generate internal excitation (it was static and time domain). The switch to dynamic response has advantages; the non-linearity of the system ramps up quickly from zero externally applied load to even small, applied loads. It avoids amplitude bandwidth limitations and drift. It offers some force dof (for example external moment loads) improved resolution by averaging over multiple measurement modes.

The 2nd prototype was only tested for 3 degrees of freedom forces (axial and two moments). The goal was to determine that non-linearity frequency shift could be used to measure externally applied loads. It was tested to a significantly high amplitudes and it was also tested with thermal gradient across its diameter.

The third prototype was tested for all 6 force modes but only tested for a small amplitude torsion load. The 3rd prototype testing was aimed at establishing the ability to excite torsion, using cross axis effect of piezo action. It has been used here to help demonstrate the near linearity of the first housing mode.

TABLE III Frequency and Shape Results for FE and Test Results for 2nd & 3rd Prototype

2nd Prototype			3rd Prototype		
FE Freq	Test Freq	shape	FE Freq (asjup1)struts pinned	Test Freq	Shape, Eff Mass Fraction
271	250	1st upper plate	736	680	Axial, T3=.3
306	302	Upper plate rot	739	530-540	R2=.064
306		Upper plate rot	739	625-640	R1=.064
497	440	Tube rotation	1157	1060	R3=.056
645	600	Piston in housing			
699		Upper plate saddle	1160		Mom+Sh
699		Upper plate saddle	1160		Mom+sh
1206	950	Upper plate rotation			
1206		Upper plate rotation			
1584	1377	Bottom plate mode	1262	1266-1268	Bottom plate, T3=.1
1658	1547	Upper plate	1967		Mom+Sh; saddle
1658		Upper plate	1967		Mom+Sh; saddle?
1817	1900.	Housing & plate	3015		Ld plate near struts
1817			3117		T1=.07; sh in X; R2=.13
			3117		T2=.07;sh in Y;R1=.13

Conclusions

The goal of this review was to identify a linear mode within our non-linear structure. There had been no interest in identifying such a capability, while design, analysis and test of the prototypes were being executed. But it has become obvious that such a capability offers a unique capability in understanding the nature of payload being handled, and to distinguish between frequency change to due applied load, vs to tip mass change.

A next stage in the development of this sensor should be an improved FE analysis of the impact of the piezo within the structure, on both linear and non-linear modes, prior to design of another version. The 3rd prototype needs additional testing – particularly for higher load levels, but also with improved instrumentation and more care with external boundary conditions. It would be used to validate the special purpose FE model.

There is still much scope for testing the 3rd prototype.

There is clearly a complicated calibration requirement, that suggests some form of artificial intelligence – probably integrated as part of a small, specialized finite element model. All sensors produced with this approach would require calibration testing.

There are additional higher frequency linear modes, which we have test records for, but future design and analysis would be more careful in establishing their characteristic's, particularly as they might apply for robotic payloads.

References

Draisey, Elzeki, Jones & Marks, 1985. *Modal Testing of the Olympus Development Model Stowed Solar Array.* s.l., www.goodvibrationsengineering.com/OlympusPaper.pdf.

Draisey, Mullins & Yiannacouras, 2001. *Progress Review Meeting for ESA*. Nobleton(Ontario): s.n.

Draisey, Mullins, Yiannacouras & Didot, 2003. *Development of Low Frequency Force Moment Sensor using Piezoceramic Elements.* Montreal, s.n., p. 283.

Draisey, S., 2003. *Space Robotic Force Moment Sensor: Boundary Condition Influences*. Montreal, www.goodvibrationsengineering.com/cctomm.pdf.

Draisey, S., 2016. *Force Moment Sensor.* United States of America, Patent No. US Patent 9,513,179 B2 Application No 14/601,012.

Draisey, S., 2018. *Excitation for 6 Degrees of Freedom Space Robotic FMS.* [Online] Available at: www.goodvibrationsengineering.com/fms3rd.pdf

Draisey, S., 2020. *4th Quarter Technical Memo STDP 5.2: FMS Dynamic Testing of 3rd Prototype,* King City, ON: s.n.

Draisey, S., 2020. *Participation Factors for Poled Piezo Ceramic under Dynamic Loading*. [Online].

UAI, 1999. CBAR bulk data. In: *UAI NASTRAN 20.1 USER"S REFERENCE MANUAL*. Torrance California: Universal Analytics, pp. 7-41 to 7-42.